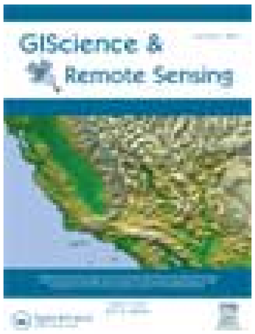

Taylor & Francis
Taylor & Francis Group

GIScience & Remote Sensing

ISSN: 1548-1603 (Print) 1943-7226 (Online) Journal homepage: http://www.tandfonline.com/loi/tgrs20

Expansion dynamics of deciduous rubber plantations in Xishuangbanna, China during 2000–2010

Weili Kou, Jinwei Dong, Xiangming Xiao, Alexander J. Hernandez, Yuanwei Qin, Geli Zhang, Bangqian Chen, Ning Lu & Russell Doughty

To cite this article: Weili Kou, Jinwei Dong, Xiangming Xiao, Alexander J. Hernandez, Yuanwei Qin, Geli Zhang, Bangqian Chen, Ning Lu & Russell Doughty (2018): Expansion dynamics of deciduous rubber plantations in Xishuangbanna, China during 2000–2010, GIScience & Remote Sensing, DOI: 10.1080/15481603.2018.1466441

To link to this article: https://doi.org/10.1080/15481603.2018.1466441

Accepted author version posted online: 18 Apr 2018.
Published online: 26 Apr 2018.

GIScience & Remote Sensing, 2018
https://doi.org/10.1080/15481603.2018.1466441

Expansion dynamics of deciduous rubber plantations in Xishuangbanna, China during 2000–2010

Weili Kou[a,b], Jinwei Dong[c], Xiangming Xiao[b,d]*, Alexander J. Hernandez[e], Yuanwei Qin[b], Geli Zhang[b], Bangqian Chen[c,f], Ning Lu[a] and Russell Doughty[b]

[a]*College of Big Data and Intelligence Engineering, Southwest Forestry University, Kunming, Yunnan, 650224 China;* [b]*Department of Microbiology and Plant Biology, and Center for Spatial Analysis, University of Oklahoma, Norman, OK 73019, USA;* [c]*Key Laboratory of Land Surface Pattern and Simulation, Institute of Geographic Sciences and Natural Resources Research, Chinese Academy of Sciences, Beijing 100101, China;* [d]*Ministry of Education Key Laboratory of Biodiversity Science and Ecological Engineering, Institute of Biodiversity Science, Fudan University, Shanghai 200433, China;* [e]*Quinney College of Natural Resources, Utah State University, Logan, UT 84322-5275, USA;* [f]*Rubber Research Institute (RRI), Chinese Academy of Tropical Agricultural Sciences, Danzhou City (CATAS), Hainan Province 571737, China*

(*Received 15 August 2017; accepted 12 April 2018*)

Monoculture rubber plantations have been replacing tropical rain forests substantially in Southern China and Southeast Asia over the past several decades, which have affected human wellbeing and ecosystem services. However, to the best of our knowledge on the extent of rubber plantation expansion and their stand ages is limited. We tracked the spatiotemporal dynamics of deciduous rubber plantations in Xishuangbanna, the second largest natural rubber production region in China, from 2000 to 2010 using time-series data from the Phased Array type L-band Synthetic Aperture Radar (PALSAR), Landsat, and Moderate Resolution Imaging Spectroradiometer (MODIS). We found that rubber plantations have been expanding across a gradient from the low-elevation plains to the high elevation mountains. The areas of deciduous rubber plantations with stand ages ≤5, 6–10, and ≥11-year old were ~1.2×10^5 ha, ~0.8×10^5 ha, and ~2.9×10^5 ha, respectively. Older rubber plantations were mainly located in low-elevation and species-rich regions (500–900 m) and younger rubber trees were distributed in areas of relative high-elevation with fragile ecosystems. Economic and market factors have driven the expansion of rubber plantations, which is not only a threat to biodiversity and environmental sustainability, but also a trigger for climatic disasters. This study illustrates that the integration of microwave, optical, and thermal data is an effective method for mapping deciduous rubber plantations in tropical mountainous regions and determining their stand ages. Our results demonstrate the spatiotemporal pattern of rubber expansions over the first decade of this century.

Keywords: rubber plantations; phenology; Landsat; PALSAR; MODIS LST; stand age

1. Introduction

Rubber plantations play very important roles in both the market of natural rubber and timber supplies (Shigematsu et al. 2011). In recent decades, the rubber plantation area has increased in Southeast Asia including China, Myanmar, Malaysia, and Thailand (Li et al. 2007; Pfeifer et al. 2016). More than one million hectares of rubber plantations

*Corresponding author. Email: xiangming.xiao@ou.edu
Geli Zhang's present address is College of Land Science and Technology, China Agricultural University, Beijing, China.

have been planted and cultivated in non-traditional rubber-growing regions, generally in the species-rich lowlands (Li et al. 2007; Ziegler, Fox, and Xu 2009; Yi et al. 2014), to meet market demands in tropical Southeast Asia since 1990 (Mann 2009; Ziegler, Fox, and Xu 2009). Rubber plantations have generated substantial amounts of revenue for local communities and the government (Fox and Castella 2013). However, the resulting decrease in natural forests has led to serious environmental problems, including water shortage (Shen 2008; Tan et al. 2011; Pfeifer et al. 2016) and biodiversity loss (Li et al. 2007; Yi et al. 2014). However, a clear understanding of rubber expansion patterns and dynamics is critical to address the role of rubber plantations in these issues and in Local Land Use and Land Cover Change (LULCC). Accurate maps of rubber plantation area and stand age are needed to document the dynamics of the rubber plantation expansion that has occurred.

Field surveys and sample statistics are the traditional method used to acquire the data necessary to calculate rubber plantation area and stand ages. However, it is a time-consuming, costly, and labor-intensive approach, and the results cannot meet the demands for monitoring over large spatial domains. Evolving remote sensing technologies present opportunities to rapidly map rubber plantations and determine their stand ages on a large scale. For example, the Moderate Resolution Imaging Spectroradiometer (MODIS), Landsat, and Huan Jing-1 are important data sources for mapping rubber plantations (Li, Liu, and Huang 2011; Li and Fox 2012; Dong et al. 2013; Senf et al. 2013). Images from these optical sensors are affected by frequent cloud covers in tropical mountainous regions (Grogan et al. 2016) where rubber trees are distributed. However, microwave data with high spatial resolutions (10–50 m) have become increasingly available in recent years. In comparison to optical sensors, Synthetic Aperture Radar (SAR) can penetrate clouds and has advantages in mapping tropical forests because long wavelengths (e.g., L-band SAR) are capable of penetrating tree canopies (Baghdadi et al. 2009; Trisasongko 2017). The Phased Array type L-band Synthetic Aperture Radar (PALSAR) is such an instrument with these characteristics (Kellndorfer et al. 2010; Dong et al. 2013; Kou et al. 2015).

According to several recent studies (Li, Liu, and Huang 2011; Dong et al. 2013; Liu et al. 2013; Senf et al. 2013), three main remote sensing properties are generally used for identifying deciduous rubber plantations: spectral reflectance, texture, and phenology. Differences in vegetation spectral signatures in key phenological phases can be used to map rubber plantations. However, rubber trees tend to be mixed with tropical evergreen vegetation, which have similar spectral characteristics (Li 2011; Liu et al. 2012). Usually, rubber plantation area is overestimated or underestimated when using spectral information alone. Canopy texture has been found to be useful to discriminate rubber plantations from natural forests by object-oriented methods and tools, as rubber trees are planted in conspicuous rows (Liu et al. 2012). Texture-based approaches may misclassify rubber plantations as other plantations that have similar textures, such as tea gardens and eucalyptus (Liu et al. 2012, 2013). Due to difficulties in spectral- and texture-based methods, some researchers resort to phenology-based methods (Liu et al. 2012; Dong et al. 2013; Kou et al. 2017). Rubber trees are evergreen in their native range (about from latitude 10°N to longitude 10° S). However, they are deciduous in Southern China and Southeast Asia (latitude up to ~22° N) in order to adapt to the cold air temperature during winter (normally below 18 ºC). Therefore, phenological changes can be used for mapping deciduous rubber plantations (Dong et al. 2013; Kou et al. 2015). This method was proven effective to distinguish deciduous rubber plantations from other land cover types in Hainan (Dong et al. 2012) and a case study region in Xishuangbanna (Kou et al. 2015).

However, it is important to verify whether the phenological approach can be used in a different rubber production region that is dominated by mountainous landscapes.

Remote sensing technology also provides new opportunities to determine stand ages of forests and plantations. Landsat data are widely used sources for forest inventories, and provide realistic basis for large scale inventory and monitoring of plantations (Suratman et al. 2004; Penevareed 2014). Regression models were used to predict stand ages of rubber plantations through the relationship between Landsat imagery bands and stand ages (Suratman et al. 2004; Chen et al. 2012). The reliability of these methods depends upon the quality, quantity, and heterogeneity of in-situ data from field surveys, which limits its application to other regions at large scales. Nevertheless, developing a feasible method for mapping stand ages of rubber plantations across large landscapes is in high demands. Temporal analysis of Landsat time-series images has been successfully used for mapping forests (Lambert et al. 2013; Wang et al. 2017) and stand ages of rubber plantations in a case study that used the Land Surface Water Index (LSWI) (Kou et al. 2015).

The objectives of this study were threefold: (1) to develop a phenology-based method for mapping rubber plantations by integration of PALSAR, Landsat, and MODIS Land Surface Temperature (LST) images in the Xishuangbanna Dai Nationality Autonomous Prefecture (Xishuangbanna) region; (2) to evaluate the stand age model of deciduous rubber plantations based on time-series Landsat images; and (3) to assess the expansion dynamics of deciduous rubber plantations through analysis of their stand age distributions from 2000 to 2010.

2. Materials and method

2.1 Study area

Xishuangbanna is located in the province of Yunnan, China, with a latitude range of 21.08°N to 22.36°N and longitude of 99.56°E to 101.50°E. About 95% of the total land area in Xishuangbanna (Lu, Liu, and Luo 2011) is montane, and the elevation ranges from 370 to 2400 m above sea level (Figure 1). Xishuangbanna consists of Jinghong, Menghai, and Mengla counties. The average annual temperature varies between 18°C and 22°C. The rainy season extends from May to October, while the dry season takes place from November to April. Since the 1950s, rubber trees have been planted in Xishuangbanna. Currently, rubber planting is a main source for incomes for those living in Xishuangbanna and the local governments.

2.2. Data and preprocessing

2.2.1 MODIS LST data

This study used the nighttime (~22:30 PM from Terra and ~01:30 AM from Aqua) MODIS LST from 8-day MYD11A2 at 1-km spatial resolution in 2010 (https://lpdaac.usgs.gov) to identify the starting and ending date of stable temperatures above 10°C through an entire year because the observations at ~01:30 AM have the lowest daily temperature from MODIS sensors. The digital number values from MYD11A2 were converted to LST with centigrade unit values (Wan et al. 2002; Wan 2008). Bad observations of the LST data in a time-series were gap-filled using the linear interpolation approach. Generally, bad observations are pixels with abnormal values, which are caused by cloud covers.

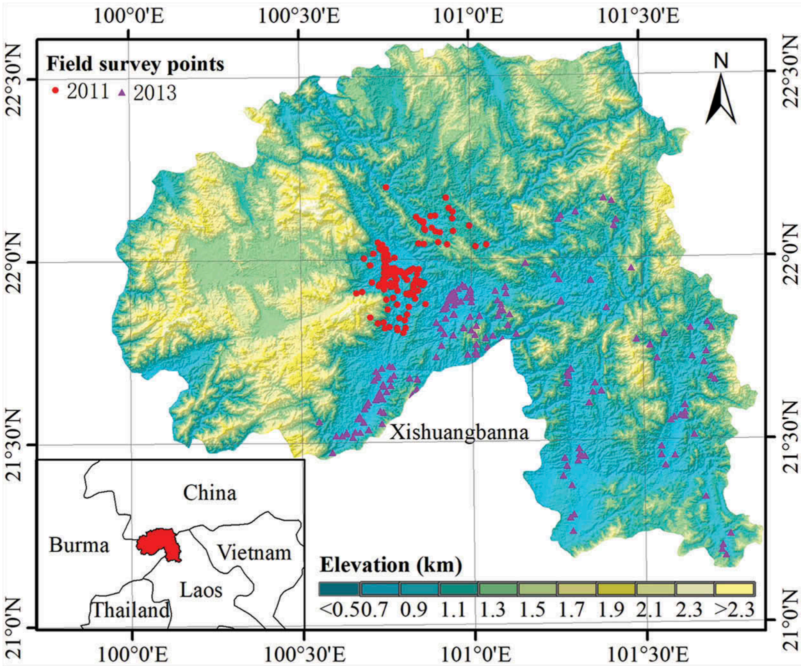

Figure 1. Xishuangbanna is located in Yunnan, China. It consists of Menghai, Jinghong, and Mengla counties and has a typical humid tropical forest environment. The red solid circles and purple solid triangles mark the locations of field survey samples of deciduous rubber plantations taken in 2011 and 2013, respectively.

2.2.2 PALSAR data

The PALSAR 50-m orthorectified mosaic data with Fine Beam Dual observational mode of 2010 was downloaded from the Earth Observation Research Center, Japan Aerospace Exploration Agency (JAXA) (http://www.eorc.jaxa.jp/ALOS/en/kc_mosaic/kc_map_50.htm) and used in this study. The dataset is organized by latitude-longitude coordinate, and each tile has 2250 columns and 2250 rows, and includes gamma-naught in HH and HV, local incidence angle, and mask information. The HH and HV data were slope-corrected and orthorectified using the 90-m Shuttle Radar Topography Mission (SRTM) Digital Elevation Model (DEM), and were also radiometrically calibrated. Due to the coarse spatial resolution of the SRTM DEM, the geometric accuracy of PALSAR HH and HV is about 12-m gamma-naught. These data were normalized by the realistic illumination area using the local incidence angle, and provides more uniform backscattering coefficients than sigma naught (Shimada et al. 2014).

2.2.3 Landsat imagery

Landsat 5/7 thematic mapper (TM)/ETM+ images during the leaf-off phase were used to retrieve stand ages of deciduous rubber plantations. A total of 749 standard level-1 terrain-corrected Landsat 5/7 TM/ETM+ images (path/row 130/045, 129/045, and 130/044) from 2000 to 2010 were downloaded (http://earthexplorer.usgs.gov/). This product type provides systematic radiometric and geometric accuracy by incorporating ground control points while employing a DEM of three arc second (90-m) resolution in Geographic coordinates with a WGS-84 datum for topographic accuracy. The geodetic accuracy of the product depends on the accuracy of the ground control points (from the GLS2000 dataset) and the resolution of the DEM used, and was processed by the Landsat Ecosystem Disturbance Adaptive Processing System (Vermote et al. 1997; Masek et al. 2006) and Fmask (Zhu and Woodcock 2012). All images were projected to the coordination system D_WGS_1984_Zone_47N. Normal Difference Vegetation Index (NDVI) (Tucker 1979), Enhanced Vegetation Index (EVI) (Huete et al. 2002), and LSWI (Xiao et al. 2004a, 2004b) were generated to identify the rubber plantations and evergreen forests.

2.2.4 Field data

We conducted several field surveys of land cover types in Xishuangbanna in 2011 and 2013, and the locations of plots were showed in Figure 1. We managed these field survey photos in the Global Geo-referenced Field Photo Library (Xiao et al. 2013). Based on 850 geo-referenced field photos and Google Earth (GE) platform, a random sampling method was used to acquire the points of interest (POIs). A total of 135 POIs of deciduous rubber plantations were used for conducting time-series analysis, training algorithm, and validating results.

2.3 Method

2.3.1 Method overview

We developed a workflow for mapping deciduous rubber plantations and their stand ages by integrating MODIS LST, PALSAR, and Landsat imagery (Figure 2). Three steps were taken: (1) a MODIS LST-based suitable map, a PALSAR-based forest/tree map, and Landsat-based phenology feature map of deciduous rubber plantations were generated independently; (2) the three maps were overlaid to generate a deciduous rubber plantation map; and (3) the stand ages were identified according to LSWI < 0 in the leaf-off phase using the deciduous rubber plantation map.

2.3.2 Identifying forest from PALSAR data

PALSAR reflects different backscatter characteristics on various land cover types. For instance, backscatter values of forests are higher than those of water and cropland (Wang et al. 2015). To map forest, we first used the 50-m PALSAR data (HH, HV, Ratio, and Difference images) and the decision tree method. This approach has been reported in the previous studies (Dong et al. 2013; Qin et al. 2015, 2016). The resulting product was reclassified into a forest/non-forest binary map. Second, we did further filtering of the resultant forest layer by using a majority filtering approach with a 3 by 3 window (Yuan et al. 2005). The forest map was used as a base map for identifying deciduous rubber plantations (see Section 2.3.3). Both deciduous rubber plantations and natural evergreen forests belong to the general forest class as mapped by the decision tree method (Qin et al. 2015). Third, the resultant map was resampled to 30-m to match the spatial resolution of Landsat 5/7 TM/ETM+ imagery. The 30-m forest baseline map included both rubber plantations and natural evergreen forests as a general forest category.

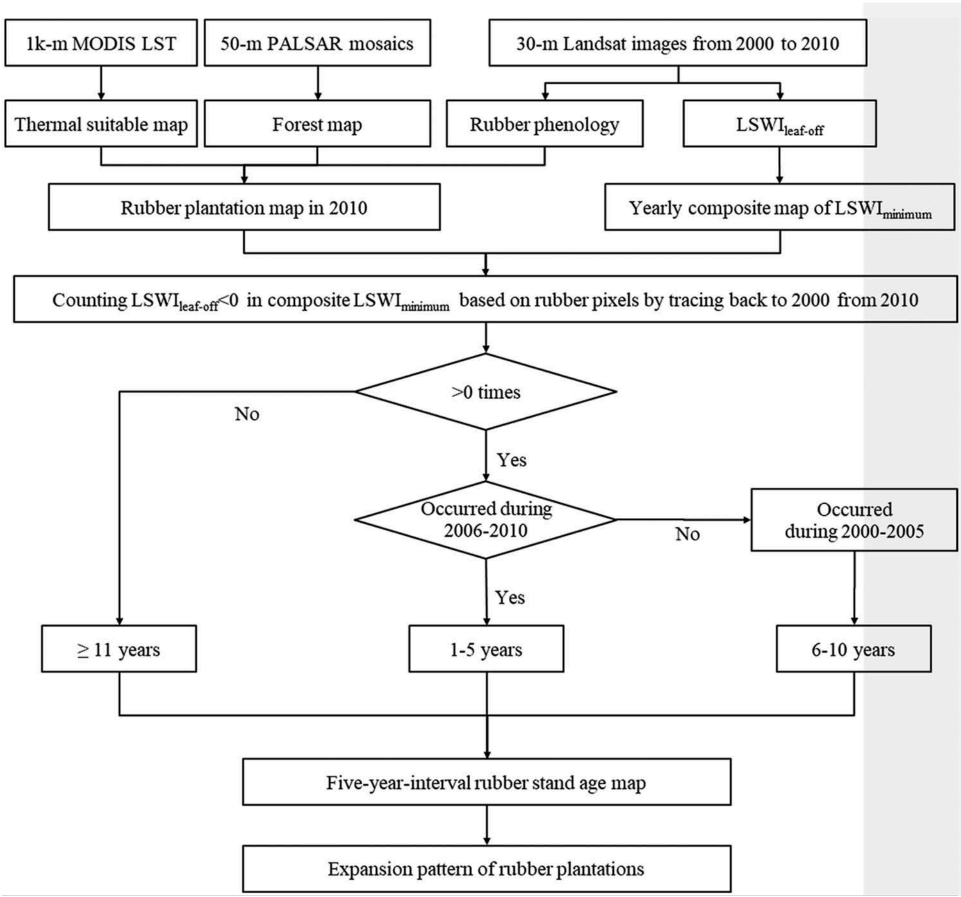

Figure 2. The workflow for mapping deciduous rubber plantations and their stand ages based on nighttime MODIS LST in 2010, 50-m PALSAR orthorectified mosaic products in 2010, and 30-m Landsat images of Xishuangbanna in 2000–2010. $LSWI_{leaf\text{-}off}$ stands for LSWI in the leaf-off phase; $LSWI_{minimum}$ is a composite LSWI image in which every pixel is the minimum of all LSWI images in the leaf-off phase.

2.3.3 Distinguishing deciduous rubber plantations from natural evergreen forest

Xishuangbanna is a tropical region where almost all native vegetation is evergreen. Rubber trees are the only deciduous trees in the study area, thus deciduous rubber plantations can be identified by changes in the spectral reflectance during the winter. There are two phenological phases (leaf-on and leaf-off) when differences in the spectral reflectance of the canopy can be captured effectively (Dong et al. 2013; Kou et al. 2015). Here, we chose the leaf-off phase to delineate rubber plantations from natural evergreen forests. However, the procedures could cause commission errors because the landscapes and ecosystems are very complex. To remedy this issue, we used additional masks based on altitude and LST data.

Low-temperature (e.g., below 10°C) can reduce rubber output and may cause serious damage to rubber trees, such as branch dieback, root rot, and death if the trees are exposed to cold temperatures for more than 20 days (Liu 2008). Regions suitable for rubber planting can be identified using the nighttime MODIS LST (Figure 3A) as those areas that are above 10°C through a year, and unsuitable regions (Figure 3B) are those that fall below 10°C in winter and spring. Thus, we determined which regions were suitable for rubber plantations using two steps. First, we identified the starting and ending dates that the nighttime MODIS LST was above 10°C for each pixel. Then we calculated the differences in the ending and starting dates for each pixel, and generated a difference map with the number of days in a year that nighttime MODIS LST was continuously higher than 10°C in 2010. A high pixel value indicates that the area is highly suitable for rubber planting. Second, we classified pixels with values of ≤48 days as areas unsuitable for cropping rubber plantations. We set this threshold by considering the accumulated low-temperature tolerance of rubber trees. By applying the threshold to the difference map, a thermal suitability map (Figure 4) for rubber trees was generated and resampled into 30 m using the nearest neighbor method (Park and Chung 2016) to match the Landsat imagery.

In addition to temperature, elevation is another important factor for rubber planting in Xishuangbanna. The 90-m DEM of Xishuangbanna was downloaded from the United States Geological Survey (USGS) and resampled to match the 30-m Landsat data using the nearest neighbor sampling method. According to the rubber planting technical specifications of Xishuangbanna, lower elevation regions (less than 950 m) are the most suitable region for planting rubber trees (Chen et al. 2016). However, to maximize revenue, some small landowners cultivate rubber trees in unsuitable elevation gradients higher than 950 m. Thus, we used ≤1500 m as an elevation threshold to further improve the LST-based thermal suitability map. The thermal suitable areas and the zones below 1500 m were used together as masks to refine the initial deciduous rubber plantation maps.

2.3.4 Mapping stand ages based on time-series Landsat images between 2000 and 2010

The timings of rubber tree leaf-off varied among the different rubber tree stands in Xishuangbanna. Three rubber plantation sites (Figure 5A–C) on different Julian Dates 018, 050, 066, and 114 in 2009 were extracted from TM/ETM+ images (R/G/B 5/4/3). The depth of purple color indicated the intensity of leaf-off. Each site had four Landsat TM/ETM+ images on

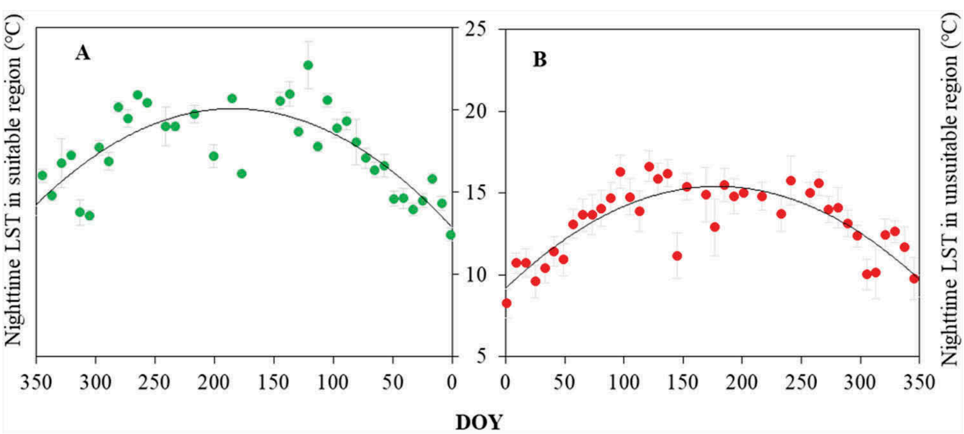

Figure 3. Temporal profiles of nighttime MODIS LST in 2010 for a suitable region (A) and an unsuitable region (B) for rubber plantation. DOY is the day of year.

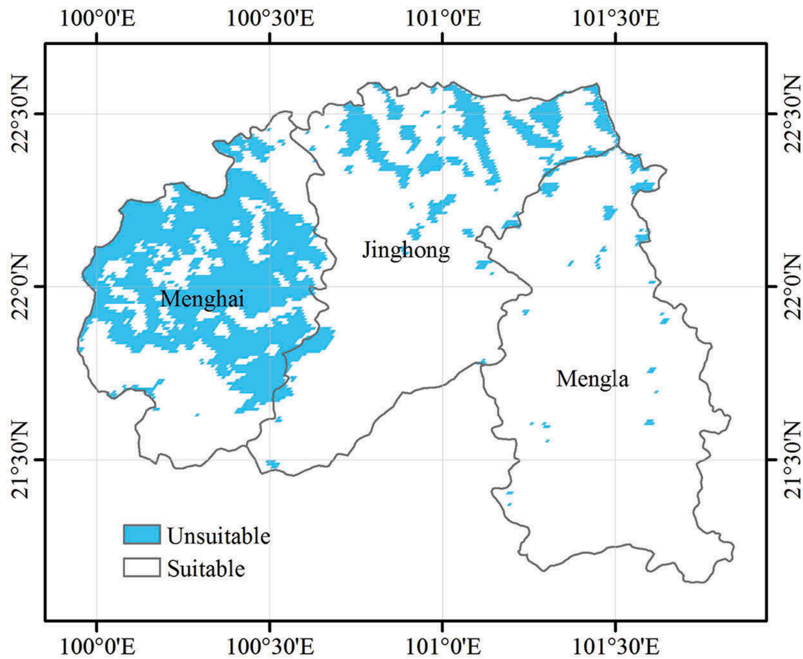

Figure 4. The thermal suitability map for growing deciduous rubber plantations in Xishuangbanna Yunnan, China in 2010 was created based on 1-km nighttime MODIS LST data.

Julian Dates 018, 050, 066, and 114 in 2009. The most intense leaf-off timings for site A, B, and C (Figure 5) were 018, 050, and 066, respectively. This difference suggested that using the LSWI minimum in leaf-off phase could get more accurate phenological characteristics. Due to various leaf-off timings of rubber trees in different environments (Figure 5), these Landsat images were composited by minimum LSWI values over all LSWI layers during the leaf-off phase in a year, and then annual minimum LSWI composite images were generated.

Based on these composited images, $LSWI_{leaf\text{-}off} < 0$ ($LSWI_{leaf\text{-}off}$ stands for LSWI in the leaf-off phase) was chosen as the threshold for stand age prediction of deciduous rubber plantations (Kou et al. 2015) and the algorithm details were shown in Figure 2. To identify deciduous rubber plantation stand ages, Landsat time-series LSWI over 2000–2010 were used to detect the year that forests were clear-cut. Figure 6 showed the temporal changes of NDVI, EVI, and LSWI at one Landsat pixel point at latitude of 21.76°N and longitude of 100.91°E where natural forest was converted into rubber plantation around 2005 (Figure 6a–c). Two key landscape images were captured from GE high-resolution imagery: 18 May 2003 (Figure 6A) and 1 May 2012 (Figure 6E). Determined by referenced data and textures, the land cover types of two images at different periods can be identified as natural forest (Figure 6D) and rubber plantation (Figure 6E). Observed from Landsat image time-series (Figure 6A–C), a sudden decline in NDVI, EVI, and LSWI appeared in 2005, which means the conversion from natural forests to rubber plantations were occurred in 2005. The LSWI value was only negative in clear-cut fields and newly cultivated rubber plantations (about between 2005 and 2010), so $LSWI_{leaf\text{-}off} < 0$ was chosen as the threshold value for stand age predictions of deciduous rubber plantations. The stand age of a deciduous rubber plantation pixel in 2010 was identified using the following steps. First, we recorded the year when $LSWI_{leaf\text{-}off} < 0$ first occurred between 2000 and 2010 (10 years). This year was considered to be the planting year of rubber

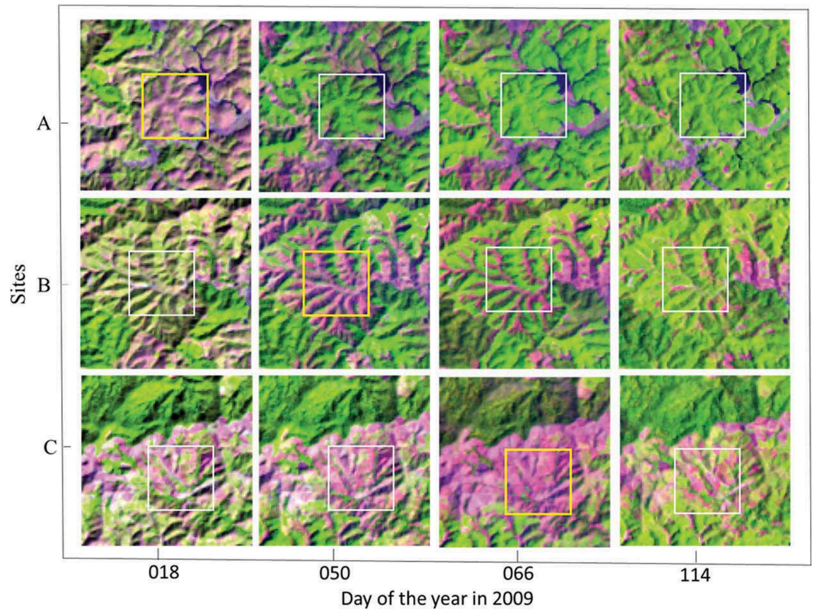

Figure 5. Leaf-off timing differences of deciduous rubber plantations in different environments during the phenological phase in Xishuangbanna. The squares mark the regions of interest of deciduous rubber plantations, with the yellow squares representing the period with the most leaf-off.

trees. Second, we grouped and reported the resultant stand ages into two age groups (≤5 and 6–10 years). Third, those rubber pixels that did not have any observations with $LSWI_{leaf\text{-}off} < 0$ during 2000–2010 were considered to be ≥11 years, given that the typical life span of rubber trees was 25–30 years.

2.3.5 Accuracy assessment of deciduous rubber plantation maps

The validation process was as follows: (1) we validated the 30-m rubber plantation map using the geo-referenced field photos from the Global Geo-referenced Field Photo Library (http://www.eomf.ou.edu/photos) and GE high-resolution images, which included randomly selected deciduous rubber plantation ROIs (5067 pixels) and non-rubber forest ROIs (1624 pixels); (2) we validated the stand age map using the National Land Resource Inventory (NLRI) data of China provided by local governments, which contained stand age data for deciduous rubber plantations. To be consistent with the resultant stand age map, NLRI was grouped into ≤5, 6–10, and ≥11 year-old categories, and different stand age ROIs (3047, 2055, and 2502 pixels) were, respectively, created corresponding to three age groups. Two confusion matrices were built to validate the deciduous rubber plantation extent map and stand age map in 2010.

2.3.6 Expansion patterns of deciduous rubber plantations from their stand ages

The expansion dynamics of deciduous rubber plantations along the elevation gradient were analyzed based on the Landsat-based stand age map at 30-m spatial resolution. First, an elevation classification system with nine categories was defined with a 100-m interval.

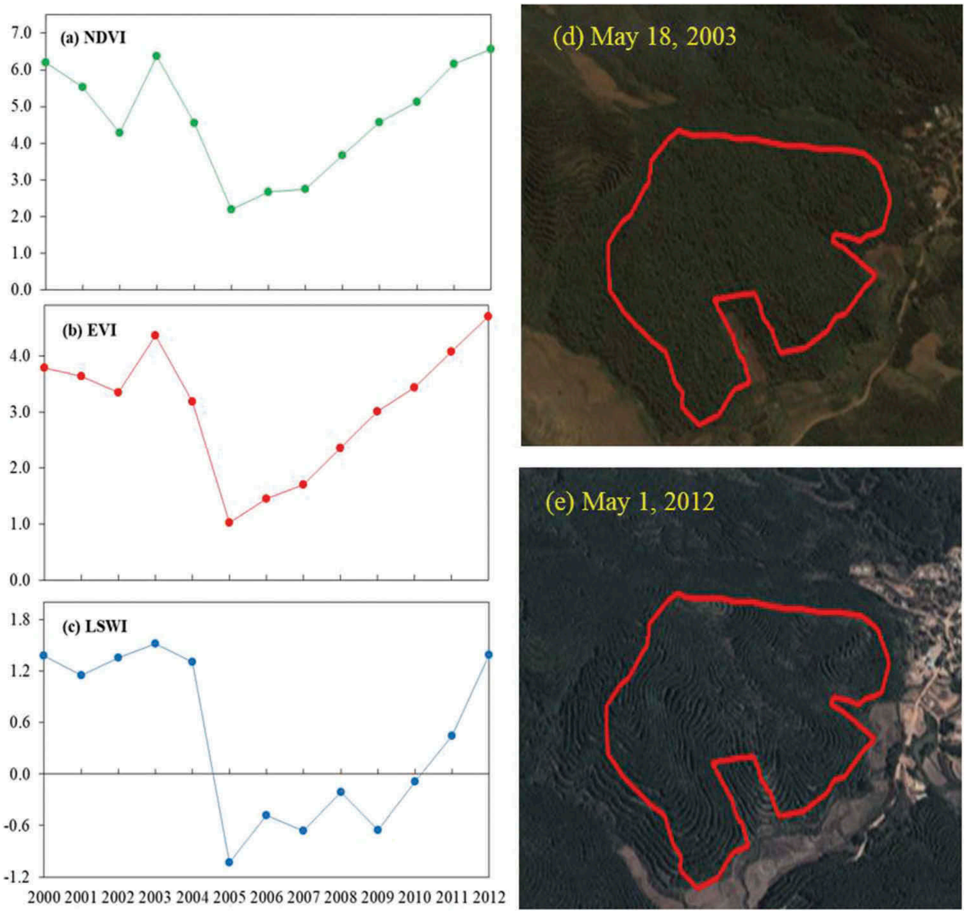

Figure 6. The time-series profile analysis of deciduous rubber plantation NDVI, EVI, and LSWI at one point with latitude of 21.76°N and longitude of 100.91°E. The points of (A), (B), and (C) are vegetation index minimums during the leaf-off phase. Two images of the same ROI outlined by red lines extracted from GE high-resolution imagery. On 18 May 2003 the ROI is native forest (D) and on 1 May 2012 the ROI is rubber plantation (E).

Second, the classified elevation gradient layer was overlaid over the stand age map of deciduous rubber plantations and pixels at each elevation zone were counted. Third, expansion patterns of deciduous rubber plantations were analyzed, and based on the statistical results we formed reasonable explanations of such patterns by examining the local LULCC policies and rubber prices records.

3. Results

3.1 Deciduous rubber plantation map of Xishuangbanna in 2010

We generated the forest and non-forest map (Figure 7) by using the PALSAR data and the decision tree method as described in previous studies (Kou et al. 2015). Based on this forest map, a deciduous and non-deciduous forest map (Figure 8A) was generated using a phenology-based mapping method as stated in Section 2.3.3. A resampled 30-

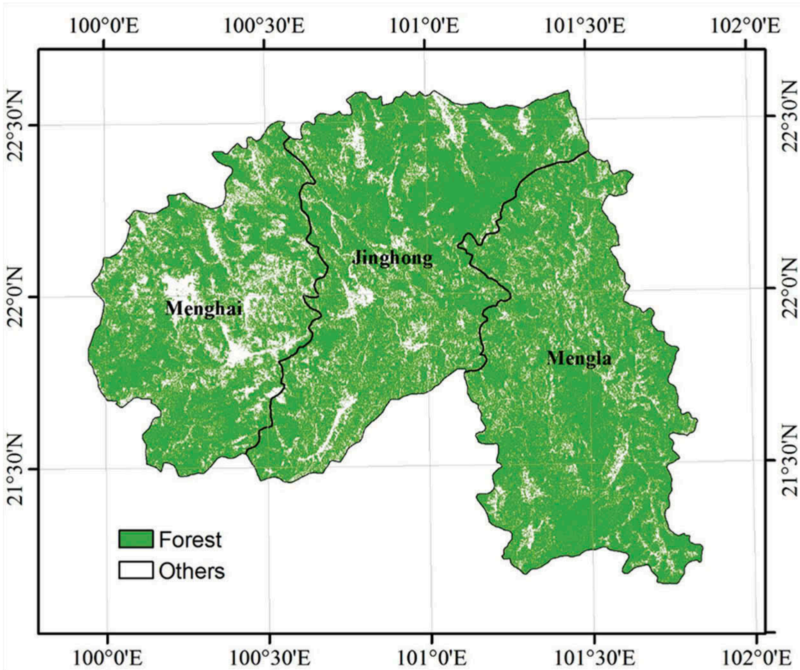

Figure 7. The resampled 30-m forest map generated from 50-m PALSAR mosaics of Xishuangbanna in 2010.

m MODIS-based thermal suitability map (Figure 8B) was generated to trim the area where the temperature is not sufficient for rubber tree growth. According to the thermal suitability map, the most suitable regions are located in Jinghong and Mengla counties.

The resultant rubber plantation map was shown in Figure 8C. The total area of deciduous rubber plantations in 2010 was estimated as ~4.9 × 10^5 ha. The overall accuracy of the resultant map is 95% and the confusion matrix is in Table 1.

3.2 Stand age map of deciduous rubber plantations of Xishuangbanna in 2010

The stand age map of deciduous rubber plantations of Xishuangbanna in 2010 is shown in Figure 9. The areas with ≤5, 6–10, and ≥11 year-old rubber plantations were, respectively, estimated as ~1.2 × 10^5 ha, ~0.8 × 10^5 ha, and ~2.9 × 10^5 ha. According to the validation results (Table 2) built from ROIs, the overall accuracy was 85%. The user's accuracies of ≤5, 6–10, and ≥11 year-old are 89%, 74%, and 89%, respectively. The producer's accuracies are 93%, 80%, and 79%, respectively. Three stand age groups of deciduous rubber plantations (≤5, 6–10, and ≥11 year-old) are radially distributed inside out, as illustrated by the stand age map of Xishuangbanna in 2010. That is, the outside is the ≤5, the middle is 6–10, and the inside is ≥11 year-old rubber trees. This indicates rubber plantations continuously expand between 2000 and 2010.

Figure 10 shows the distribution characteristics of stand ages of deciduous rubber plantations of Xishuangbanna in 2010 at different elevation gradients. Rubber plantation mainly ranges from 500 to 1300 m. The rubber plantations ≥11 year-old were mainly

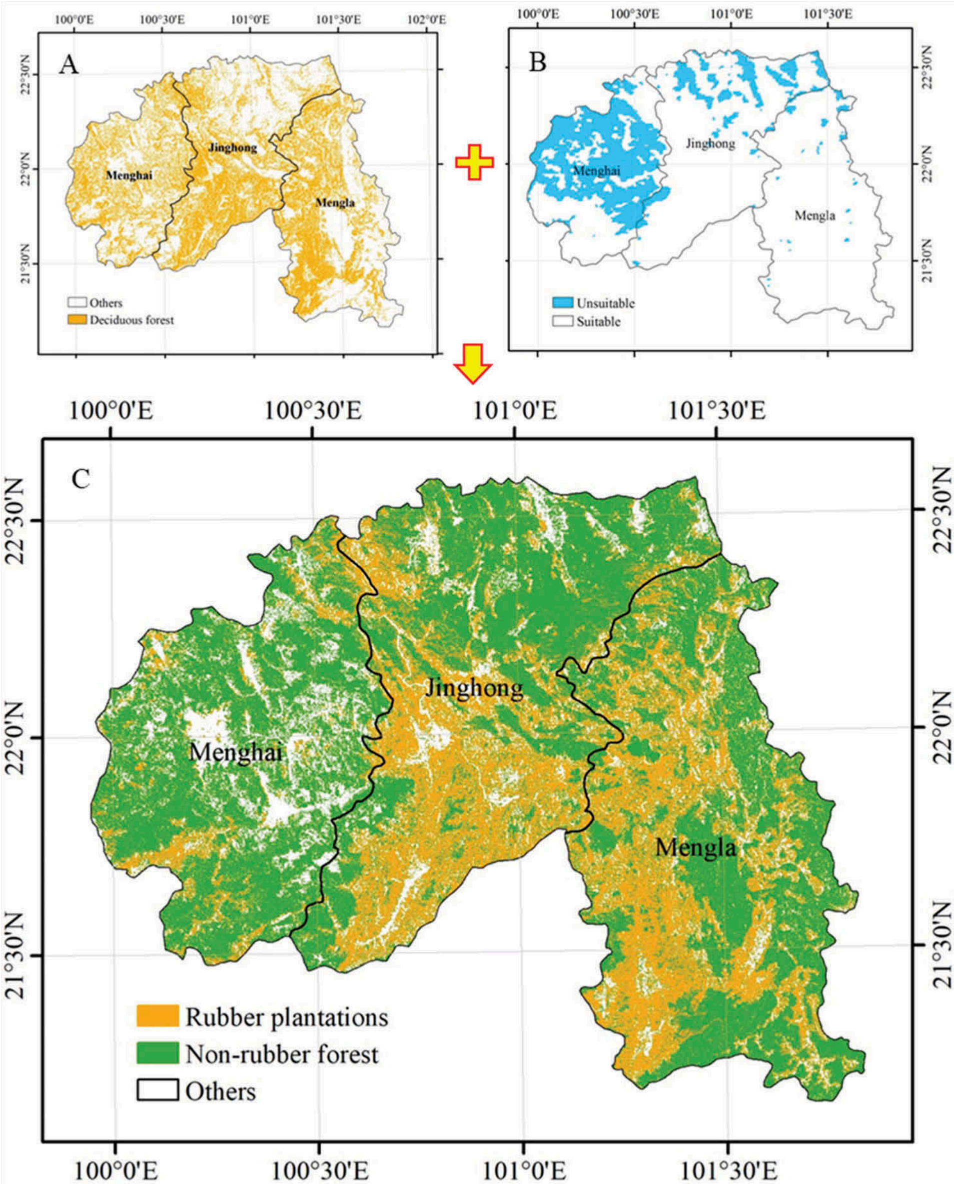

Figure 8. The rubber plantation map of Xishuangbanna in 2010. (A) Deciduous/non-deciduous forest map generated from resampled 30-m PALSAR-based forest map and the phenological characteristics. (B) Suitable region map for growing rubber plantations based on resampled 30-m MODIS LST. (C) Deciduous rubber plantation map by overlaying (A) with (B).

located in low-elevation regions (500–900 m), most of those ≤5 year-old are at relatively high-elevation (1000–1200 m), and 6–10 year-old stands have a slightly higher density at 800–1000 m than other elevation gradients. Our results indicated that rubber plantations have transitioned from low- to high-elevation gradients.

Table 1. Accuracy assessment (confusion matrix) of the 30-m deciduous rubber plantation map of Xishuangbanna in 2010. The overall accuracy is 95%.

Classes	Rubber plantation	Non-rubber forest	Total pixels	User's accuracy
Rubber plantations	4878	189	5067	96%
Non-rubber forest	114	1510	1624	93%
Total pixels	4992	1699	6691	
Producer's accuracy	98%	89%		

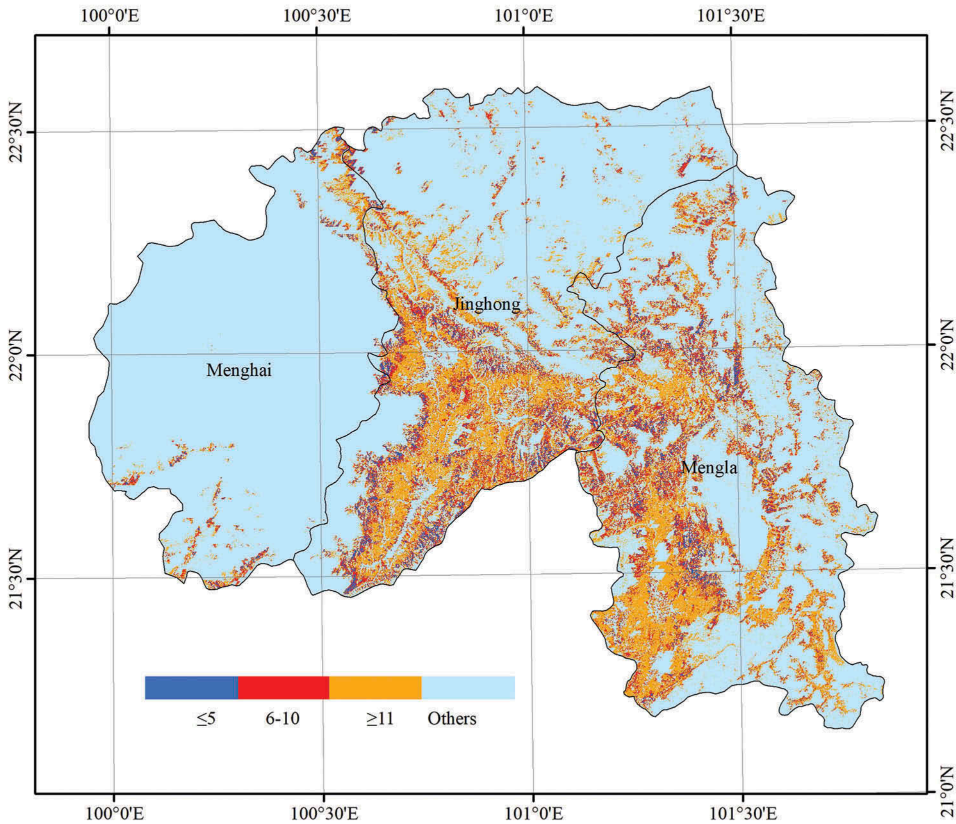

Figure 9. A 5-year-interval stand age map (≤5, 6–10, and ≥11-year old) of deciduous rubber plantations at 30-m spatial resolution of Xishuangbanna in 2010 was generated based on 30-m inter-annual composite Landsat images between 2000 and 2010 by $LSWI_{leaf\text{-}off} < 0$.

4. Discussion

4.1. Advantages in the integration of MODIS LST, PALSAR, and Landsat imagery

Currently, integration of multi-sensor data for LULCC studies is an important research topic. Previous studies have reported the rubber plantation mapping efforts by integrating PALSAR and MODIS (Dong et al. 2012), Landsat and MODIS (Liu et al. 2013), as well as PALSAR and Landsat (Kou et al. 2015). PALSAR backscatters could contribute to separation of different plantation species like rubber trees, oil palm, coconut, and wattles (Miettinen and

Table 2. Accuracy assessment (confusion matrix) of the resultant stand age map was conducted using the 30-m Landsat images of Xishuangbanna, Yunnan, China in 2010. The overall accuracy is 85%.

Classes	≤5 yrs	6–10 yrs	≥11 yrs	Total pixels	User's accuracy
≤5 years	2711	129	207	3047	89%
6–10 years	165	1519	371	2055	74%
≥11 years	39	246	2217	2502	89%
Total pixels	2915	1894	2795		
Producer's accuracy	93%	80%	79%		

Liew 2011), especially in humid tropical regions with frequent cloud covers (Dong et al. 2012, 2013). Microwave-based remote sensing platforms such as PALSAR have the advantage of being able to penetrate clouds, while optical sensors are limited by cloud cover and adverse weather conditions, especially in tropical and subtropical regions.

PALSAR was used to obtain a forest mask to exclude land cover types that usually mix with rubber plantations including tea gardens and shrubs (Liu et al. 2012). PALSAR L-band collects useful data around-the-clock under any weather conditions, and can identify forests higher than 5 m in height. Given that the average height of tea gardens (except Arbor teas) is ~0.8–1.2 m and of shrubs is ~0.9–2.5 m, most of these communities can be excluded from deciduous rubber plantation maps using PALSAR data. This study demonstrates these benefits from PALSAR in mapping deciduous rubber plantations in tropical mountain regions. Although this study used 50-m PALSAR images, free PALSAR imagery with fine spatial resolution (25 m) have been recently released. This new data presents more opportunities for the application of our algorithm in the near future. However, PALSAR mosaics may omit some 1–2 year-old rubber trees which are shorter than 5 m, and include some Arbor tea trees (~15–30 m) taller than 5 m.

According to recent research, spectral, textural, and phenological approaches were used to map deciduous rubber plantations in Xishuangbanna (Liu et al. 2012; Dong et al. 2013; Senf et al. 2013; Kou et al. 2015). However, rubber plantations were still prone to being misclassified as natural forests, tea gardens, or shrubs. We overcame most of these issues by integrating all three approaches with PALSAR, Landsat, and MODIS data. The growth of rubber trees needs strict thermal conditions, so we used MODIS LST data to identify areas that are suitable for planting deciduous rubber plantations. MODIS LST was used instead of air temperature because the remote sensing based LST data has higher spatial resolution than the interpolated meteorological data from the small number of weather stations in the study area. The suitable thermal map was generated using the 8-day MODIS LST data at 1 km spatial resolution. We used a revisiting unit (8 days) as a threshold to identify the suitable regions where nighttime MODIS LST is continuous lower than 10°C. The suitable thermal mask reduced commission errors of our rubber plantation map.

4.2 Implications of upward expansion of deciduous rubber plantations in mountains

The pattern of rubber expansion is very important for making land management decisions and local land use policies. We found that the younger stand ages of deciduous rubber plantations were occurring at higher elevations in Xishuangbanna. This expansion gradient was driven by local land use policies, economic development, and environment

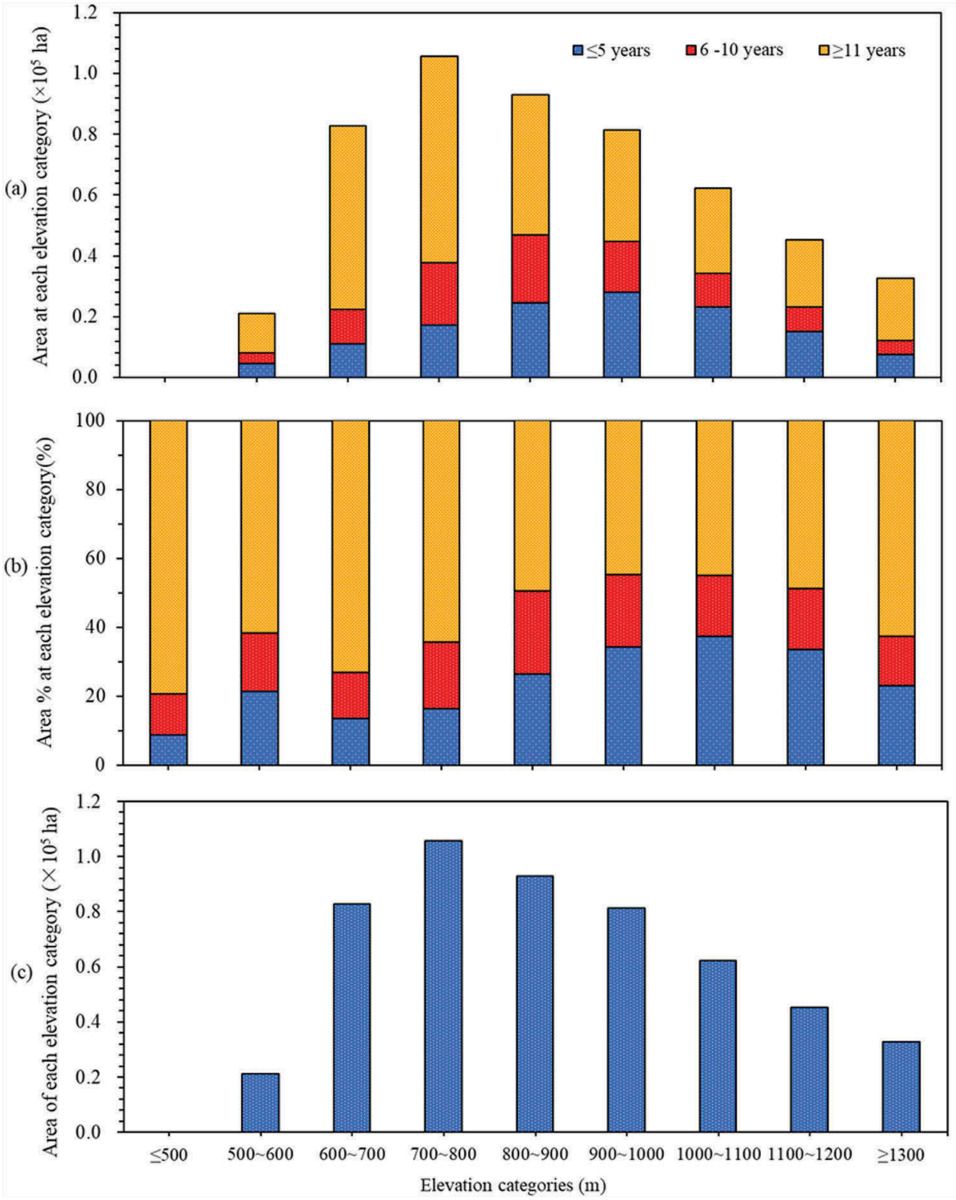

Figure 10. Elevation distribution characteristics are in area (a), area % (b), and total area (c) for different stand age groups of deciduous rubber plantations of Xishuangbanna in 2010.

limitations, and agreed with the results from previous studies (Li et al. 2007; Liu et al. 2013). The distribution reflects environmental degradation due to rubber production demands. Rubber plantations are more productive at the lower elevations, so land owners and local governments can get more revenue from low-elevation plantations (Yi et al. 2014). However, the most suitable croplands and native rainforests are also distributed in these lower regions (Li et al. 2007; Li, Liu, and Huang 2011; Yi et al. 2014). In recent years, strict cropland and natural forest protection policies limited the expansion of rubber plantations at low-elevation. Although protection policies are tight, farmers still seek new spaces for rubber planting due to the profitability.

The continual increase of natural rubber prices (Figure 11) agreed well with the increase in rubber plantation area from 2000 to 2010. Figure 11 illustrates the long-term price index for technically specified rubber (TSR-20) blocks, including the boom cycle that began in 2002–2003, which was interrupted by a brief correction in 2008–2009. The historical maximum price index (660) was achieved in 2011, the year after the index decreased by almost 1/3 (470). In the 1950s, rubber trees were cultivated at Xishuangbanna and managed by state farms. Lowland regions with high air temperature were the most suitable areas and were early exploited for cultivating rubber plantations by state farms in the development of the natural rubber industry. Rubber plantations in these areas were planted relatively early, so ≥11 year-old rubber plantations dominate these regions. The dramatic increase in the global price of natural rubber in 2002–2003 (Khin et al. 2008) provided incentives of rubber tree planting for smallholders, including private enterprises and farmers. Thus, most of the 6–10 year-old rubber plantations were planted between 2000 and 2005 by smallholders near to the state farms. With the rubber planting reaching saturation in low-elevation areas, the smallholders sought more planting space in relatively high-elevation regions. The improvement in the rubber tree cultivar also contributed to the transition of rubber trees into the relative higher elevation regions in recent years. Hence, the ≤5 year-old rubber trees were planted at higher elevations than the original rubber plantations, which mean that some rubber plantations were being created at the expense of the native tropical forests.

Rubber plantations occur over a very wide elevational range from 500 to 1300 m (Figure 10), which indicates that natural forest and other land cover types (such as cropland) have been converted into monoculture rubber plantations. This distribution implies that regional biodiversity has been substantially disturbed across a wide

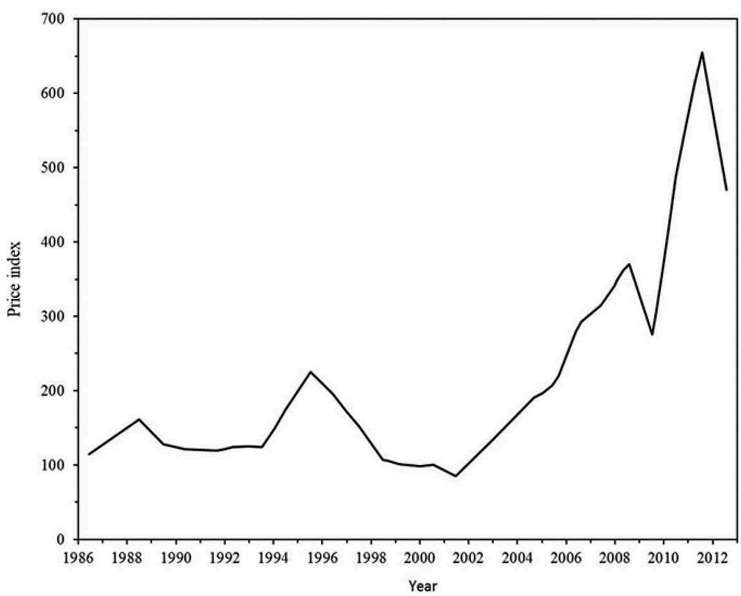

Figure 11. Annual free market rubber price index for TSR-20 grade rubber between 1986 and 2012.

elevational gradient, which may cause the loss of forest species (Ferreira et al. 2016) and forest ecosystem services, such as regional biogeochemical nutrient cycling and animal habitat for species such as the Asian Elephant (*Elephas maximus*) and tiger (*Panthera tigris*) (Li et al. 2007). Foggy days are a very important indicator of ecosystem health in tropical regions. However, due to dramatic increases in rubber plantation area in recent years, foggy days have substantially decreased by about one third since 1950s (Zhu et al. 2004).

4.3 Advantage of best available pixels of all landsat images used in key phenological phases

Compared to previous studies (Li, Liu, and Huang 2011; Dong et al. 2013), our method utilizes the phenological approach by using all good-quality Landsat images available, as shown in Figure 5. Previous studies (Dong et al. 2013) used one scene good-quality Landsat image in the phenological phases (leaf-on or leaf-off) to delineate deciduous rubber plantations from forests. However, we used the best available pixels of Landsat images taken during the leaf-off phase and all bad observations were identified and discarded according to the Fmask flag or our algorithms. We developed a pixel-based algorithm to generate a composite image in which each pixel is the lowest value of all LSWI products at the same location in the leaf-off phase. This strategy also could be applied to map rubber plantations during the leaf-on phase, but the highest value should be used. For the stand age extraction, we found that $LSWI_{leaf\text{-}off} < 0$ was suitable, while other reflectance bands or vegetation indices (such as NIR, NDVI, or EVI) may also work.

4.4 Sources of uncertainty and limitations

We anticipated that commission errors in the identification of suitable regions for cropping rubber plantations would come from using nighttime MODIS LST due to its coarse spatial resolution (1 km), and from the differences between LST and air temperatures. The study area in the tropics is frequently covered by clouds and their shadows, and Landsat has a relatively rough temporal resolution (16 days), thus there were not enough Landsat images to generate a consistent time-series for monitoring rubber plantations. Due to the number limited number of weather stations in the study area and its mountainous topography, the interpolation of the weather station data would be coarser than the MODIS LST data.

Although the Landsat imagery was processed using the Fmask algorithm, the quality of the data used in this study was limited by clouds, cloud shadows, and mountain shadows, which likely generate outliers in the NDVI, EVI, or LSWI datasets. We used the best available pixels of all Landsat images in the leaf-off phase, so such errors were limited.

Long-term and high-quality remote sensing images in two key phenological phases (leaf-off or leaf-on) were used for time-series analysis of deciduous rubber plantations, but the availability of good-quality observations may limit the application of our phenology-based algorithm. For example, leaf-off and leaf-on occurs during a relatively narrow range of ~3 months and not be captured due to frequent cloud cover and cloud shadows (Kou et al. 2015). Thus, the number of high-quality Landsat images is a potential constraint for the application of our algorithm.

The method we developed in this study mainly focuses on mapping rubber plantations and their stand ages outside of their native range at a latitude range of ~≥21°N in Southeast Asia, and did not consider the native range of rubber trees at a latitude of ~10°S to ~10°N.

5. Conclusion

This study mapped deciduous rubber plantations and determined their stand ages in Xishuangbanna, China, in 2010 by using MODIS LST, PALSAR, and Landsat images. The combination of MODIS LST-based thermal suitable map, the PALSAR-based forest map, and time-series Landsat-based analyses improved the reliability of the results greatly. The best available pixels of all good-quality Landsat observations were used to make full use of archived optical images in the tropics. We found that the area of deciduous rubber plantations increased annually and that rubber plantations expanded from the species-rich lowlands into the ecologically fragile mountainous regions over the past decade. This study demonstrated the advantage of using multiple remote sensing sources in mapping deciduous rubber plantations, which reduced errors from mixed pixels, clouds and cloud shadows, and produced highly accurate deciduous rubber plantation and stand age maps. Locally, some farmers clear-cut natural forest for rubber planting. Rubber plantations are now distributed in a very wide range of elevations (roughly from ~500 to ~1300 m), which may destroy the biodiversity of Xishuangbanna and may cause losses in ecosystem services. This detailed information about the spatial distribution stand ages of deciduous rubber plantations are helpful for further studies on forest planning, forest management, biogeochemical nutrient cycling, and ecosystem assessment.

Disclosure statement

No potential conflict of interest was reported by the authors.

Funding

This work was supported by the National Natural Science Foundation of China [31760181], [31400493]; the Strategic Priority Research Program of the Chinese Academy of Sciences (CAS) [XDA19040301]; Key Research Program of Frontier Sciences of CAS [QYZDB-SSW-DQC005]; the US NASA Land Use and Land Cover Change program [NNX14AD78G]; the Joint Special Project of Yunnan Provincial Agricultural Basic Research of China [2017FG001(-034)]; the Science Research Fund of Yunnan Provincial Education Department, China [2014Y324]; and the US National Science Foundation (NSF) EPSCoR program [NSF-IIA-1301789].

ORCID

Alexander J. Hernandez http://orcid.org/0000-0001-7690-002X

Bangqian Chen http://orcid.org/0000-0003-0209-4285

Russell Doughty http://orcid.org/0000-0001-5191-2155

References

Baghdadi, N., N. Boyer, P. Todoroff, M. El Hajj, and A. Bégué. 2009. “Potential of SAR Sensors Terrasar-X, Asar/Envisat and PALSAR/ALOS for Monitoring Sugarcane Crops on Reunion Island.” *Remote Sensing of Environment* 113 (8): 1724–1738. doi:10.1016/j.rse.2009.04.005.

Chen, B. Q., J. H. Cao, J. K. Wang, Z. X. Wu, Z. L. Tao, J. M. Chen, C. Yang, and G. S. Xie. 2012. "Estimation of Rubber Stand Age in Typhoon and Chilling Injury Afflicted Area with Landsat Tm Data: A Case Study in Hainan Island, China." *Forest Ecology and Management* 274: 222–230. doi:10.1016/j.foreco.2012.01.033.

Chen, B. Q., X. P. Li, X. M. Xiao, B. Zhao, J. W. Dong, W. L. Kou, Y. W. Qin, et al. 2016. "Mapping Tropical Forests and Deciduous Rubber Plantations in Hainan Island, China by Integrating PALSAR 25-M and Multi-Temporal Landsat Images." *International Journal of Applied Earth Observation and Geoinformation* 50: 117–130. doi:10.1016/j.jag.2016.03.011.

Dong, J. W., X. M. Xiao, B. Q. Chen, N. Torbick, C. Jin, G. L. Zhang, and C. Biradar. 2013. "Mapping Deciduous Rubber Plantations through Integration of PALSAR and Multi-Temporal Landsat Imagery." *Remote Sensing of Environment* 134: 392–402. doi:10.1016/j.rse.2013.03.014.

Dong, J. W., X. M. Xiao, S. Sheldon, C. Biradar, and G. S. Xie. 2012. "Mapping Tropical Forests and Rubber Plantations in Complex Landscapes by Integrating PALSAR and MODIS Imagery." *ISPRS Journal of Photogrammetry and Remote Sensing* 74: 20–33. doi:10.1016/j.isprsjprs.2012.07.004.

Ferreira, M. P., M. Zortea, D. C. Zanotta, Y. E. Shimabukuro, and C. R. De Souza Filho. 2016. "Mapping Tree Species in Tropical Seasonal Semi-Deciduous Forests with Hyperspectral and Multispectral Data." *Remote Sensing of Environment* 179: 66–78. doi:10.1016/j.rse.2016.03.021.

Fox, J. M., and J.-C. Castella. 2013. "Expansion of Rubber (*Hevea brasiliensis*) in Mainland Southeast Asia: What are the Prospects for Smallholders?" *Journal of Peasant Studies* 40 (1): 155–170. doi:10.1080/03066150.2012.750605.

Grogan, K., D. Pflugmacher, P. Hostert, J. Verbesselt, and R. Fensholt. 2016. "Mapping Clearances in Tropical Dry Forests Using Breakpoints, Trend, and Seasonal Components from MODIS Time Series: Does Forest Type Matter?" *Remote Sensing* 8 (8): 657. doi:10.3390/rs8080657.

Huete, A., K. Didan, T. Miura, E. P. Rodriguez, X. Gao, and L. G. Ferreira. 2002. "Overview of the Radiometric and Biophysical Performance of the MODIS Vegetation Indices." *Remote Sensing of Environment* 83 (1–2): 195–213. doi:10.1016/S0034-4257(02)00096-2.

Kellndorfer, J. M., W. S. Walker, J. B. Bishop, T. Cormier, A. Baccini, S. J. Goetz, N. Laporte, and F. Holecz. 2010. "Pan-Tropical Forest Cover from ALOS-PALSAR Data." In *AGU Fall Meeting Abstracts, B42D-06*. San Francisco, CA: American Geophysical Union.

Khin, A. A., E. C. F. Chong, Z. Mohammed, and M. N. Shamsudin. 2008. "Natural Rubber Price Forecasting in the World Market." Paper presented at the Agriculture Sustainability Through Participative Global Extension Agrex08 Conference (15-19 June), Bangi-Putrajaya.

Kou, W. L., C. X. Liang, L. L. Wei, A. J. Hernandez, and X. J. Yang. 2017. "Phenology-Based Method for Mapping Tropical Evergreen Forests by Integrating of MODIS and Landsat Imagery." *Forests* 8 (2): 34. doi:10.3390/f8020034.

Kou, W. L., X. M. Xiao, J. W. Dong, S. Gan, D. L. Zhai, G. L. Zhang, Y. W. Qin, and L. Li. 2015. "Mapping Deciduous Rubber Plantation Areas and Stand Ages with PALSAR and Landsat Images." *Remote Sensing* 7 (1): 1048–1073. doi:10.3390/rs70101048.

Lambert, J., C. Drenou, J. P. Denux, G. Balent, and V. Cheret. 2013. "Monitoring Forest Decline through Remote Sensing Time Series Analysis." *GIScience & Remote Sensing* 50 (4): 437–457. doi:10.1080/15481603.2013.820070.

Li, H. M., T. M. Aide, Y. X. Ma, W. J. Liu, and M. Cao. 2007. "Demand for Rubber Is Causing the Loss of High Diversity Rain Forest in SW China." *Biodiversity and Conservation* 16 (6): 1731–1745. doi:10.1007/s10531-006-9052-7.

Li, Y. F., G. H. Liu, and C. Huang. 2011. "Analysis of Distribution Characteristics of *Hevea brasiliensis* in the Xishuangbanna Area Based on HJ-1 Satellite Data." *SCIENTIA SINICA Informationis* 41 (suppl): 166–176.

Li, Z. 2011. "Rubber Tree Distribution Mapping in Northeast Thailand." *International Journal of Geosciences* 02 (04): 573–584. doi:10.4236/ijg.2011.24060.

Li, Z., and J. M. Fox. 2012. "Mapping Rubber Tree Growth in Mainland Southeast Asia Using Time-Series MODIS 250 M NDVI and Statistical Data." *Applied Geography* 32 (2): 420–432. doi:10.1016/j.apgeog.2011.06.018.

Liu, S. 2008. "Influence of the Cold Stress on Rubber Plantation at Xiqing State Farm in Hainan." *Scientia Silvae Sinicae* 44 (11): 161–163.

Liu, X. N., Z. M. Feng, L. G. Jiang, P. Li, C. H. Liao, Y. Z. Yang, and Z. You. 2013. “Rubber Plantation and Its Relationship with Topographical Factors in the Border Region of China, Laos and Myanmar.” *Journal of Geographical Sciences* 23 (6): 1019–1040. doi:10.1007/s11442-013-1060-4.

Liu, X. N., Z. M. Feng, L. G. Jiang, and J. H. Zhang. 2012. “Rubber Plantations in Xishuangbanna: Remote Sensing Identification and Digital Mapping.” *Resources Science* 34 (9): 1769–1780.

Lu, H. J., W. J. Liu, and Q. P. Luo. 2011. “Ecohydrological Effects of Litter Layer in a Mountainous Rubber Plantation in Xishuangbanna, Southwest China.” *Chinese Journal of Ecology* 30 (10): 2129–2136.

Mann, C. C. 2009. “Addicted to Rubber.” *Science* 325 (5940): 564–566. doi:10.1126/science.325_564.

Masek, J. G., E. F. Vermote, N. E. Saleous, R. Wolfe, F. G. Hall, K. F. Huemmrich, F. Gao, J. Kutler, and T.-K. Lim. 2006. “A Landsat Surface Reflectance Dataset for North America, 1990-2000.” *IEEE Geoscience and Remote Sensing Letters* 3 (1): 68–72. doi:10.1109/Lgrs.2005.857030.

Miettinen, J., and S. C. Liew. 2011. “Separability of Insular Southeast Asian Woody Plantation Species in the 50 M Resolution ALOS PALSAR Mosaic Product.” *Remote Sensing Letters* 2 (4): 299–307. doi:10.1080/01431161.2010.520345.

Park, H. S., and G. H. Chung. 2016. “Stochastic Disaggregation of Daily Rainfall Based on K-Nearest Neighbor Resampling Method.” *Journal of Korea Water Resources Association*, 49 (4): 283–291. doi:10.3741/JKWRA.2016.49.4.283.

Penevareed, E. 2014. “Understanding Land-Cover Change Dynamics of a Mangrove Ecosystem at the Village Level in Krabi Province, Thailand, Using Landsat Data.” *GIScience & Remote Sensing* 51 (4): 403–426. doi:10.1080/15481603.2014.936669.

Pfeifer, M., L. Kor, R. Nilus, E. Turner, J. Cusack, I. Lysenko, M. Khoo, V. K. Chey, A. C. Chung, and R. M. Ewers. 2016. “Mapping the Structure of Borneo’s Tropical Forests across a Degradation Gradient.” *Remote Sensing of Environment* 176: 84–97. doi:10.1016/j.rse.2016.01.014.

Qin, Y. W., X. M. Xiao, J. W. Dong, G. L. Zhang, P. S. Roy, P. K. Joshi, H. Gilani, et al. 2016. “Mapping Forests in Monsoon Asia with ALOS PALSAR 50-M Mosaic Images and MODIS Imagery in 2010.” *Scientific Reports* 6. doi:10.1038/srep20880.

Qin, Y. W., X. M. Xiao, J. W. Dong, G. L. Zhang, M. Shimada, J. Y. Liu, C. G. Li, W. L. Kou, and B. Moore. 2015. “Forest Cover Maps of China in 2010 from Multiple Approaches and Data Sources: PALSAR, LANDSAT, MODIS, FRA, and NFI.” *ISPRS Journal of Photogrammetry and Remote Sensing* 109: 1–16. doi:10.1016/j.isprsjprs.2015.08.010.

Senf, C., D. Pflugmacher, S. Van der Linden, and P. Hostert. 2013. “Mapping Rubber Plantations and Natural Forests in Xishuangbanna (Southwest China) Using Multi-Spectral Phenological Metrics from MODIS Time Series.” *Remote Sensing* 5 (6): 2795–2812. doi:10.3390/rs5062795.

Shen, R. 2008. “Rubber Trees for Tire Industry Shrink China Rainforests.” *Reuters* 6 (April): 2008.

Shigematsu, A., N. Mizoue, K. Ide, K. Khun, M. Pheng, S. Yoshida, K. Kohroki, and N. Sato. 2011. “Estimation of Rubberwood Production in Cambodia.” *New Forests* 42 (2): 149–162. doi:10.1007/s11056-010-9243-7.

Shimada, M., T. Itoh, T. Motooka, M. Watanabe, T. Shiraishi, R. Thapa, and R. Lucas. 2014. “New Global Forest/Non-Forest Maps from ALOS PALSAR Data (2007–2010).” *Remote Sensing of Environment* 155 (Supplement C): 13–31. doi:10.1016/j.rse.2014.04.014.

Suratman, M. N., G. Q. Bull, D. G. Leckie, V. M. Lemay, P. L. Marshall, and M. R. Mispan. 2004. “Prediction Models for Estimating the Area, Volume, and Age of Rubber (*Hevea brasiliensis*) Plantations in Malaysia Using Landsat TM Data.” *International Forestry Review* 6 (1): 1–12. doi:10.1505/ifor.6.1.1.32055.

Tan, Z.-H., Y.-P. Zhang, Q.-H. Song, W.-J. Liu, X.-B. Deng, J.-W. Tang, Y. Deng, et al. 2011. “Rubber Plantations Act as Water Pumps in Tropical China.” *Geophysical Research Letters* 38 (24): n/a–n/a. doi:10.1029/2011gl050006.

Trisasongko, B. H. 2017. “Mapping Stand Age of Rubber Plantation Using ALOS-2 Polarimetric SAR Data.” *European Journal of Remote Sensing* 50 (1): 64–76. doi:10.1080/22797254.2017.1274569.

Tucker, C. J. 1979. “Red and Photographic Infrared Linear Combinations for Monitoring Vegetation.” *Remote Sensing of Environment* 8 (2): 127–150. doi:10.1016/0034-4257(79)90013-0.

Vermote, E. F., N. ElSaleous, C. O. Justice, Y. J. Kaufman, J. L. Privette, L. Remer, J. C. Roger, and D. Tanré. 1997. "Atmospheric Correction of Visible to Middle-Infrared EOS-MODIS Data over Land Surfaces: Background, Operational Algorithm and Validation." *Journal of Geophysical Research: Atmospheres* 102 (D14): 17131–17141. doi:10.1029/97jd00201.

Wan, Z. M. 2008. "New Refinements and Validation of the MODIS Land-Surface Temperature/Emissivity Products." *Remote Sensing of Environment* 112 (1): 59–74. doi:10.1016/j.rse.2006.06.026.

Wan, Z. M., Y. L. Zhang, Q. C. Zhang, and Z.-L. Li. 2002. "Validation of the Land-Surface Temperature Products Retrieved from Terra Moderate Resolution Imaging Spectroradiometer Data." *Remote Sensing of Environment* 83 (1–2): 163–180. doi:10.1016/S0034-4257(02)00093-7.

Wang, J., X. M. Xiao, Y. W. Qin, J. W. Dong, G. Geissler, G. L. Zhang, N. Cejda, B. Alikhani, and R. B. Doughty. 2017. "Mapping the Dynamics of Eastern Redcedar Encroachment into Grasslands during 1984–2010 through PALSAR and Time Series Landsat Images." *Remote Sensing of Environment* 190: 233–246. doi:10.1016/j.rse.2016.12.025.

Wang, J., X. M. Xiao, Y. W. Qin, J. W. Dong, G. L. Zhang, W. L. Kou, C. Jin, Y. T. Zhou, and Y. Zhang. 2015. "Mapping Paddy Rice Planting Area in Wheat-Rice Double-Cropped Areas through Integration of Landsat-8 Oli, MODIS, and PALSAR Images." *Scientific Reports* 5: 10088. doi:10.1038/srep10088.

Xiao, X. M., D. Hollinger, J. Aber, M. Goltz, E. A. Davidson, Q. Y. Zhang, and B. Moore III. 2004a. "Satellite-Based Modeling of Gross Primary Production in an Evergreen Needleleaf Forest." *Remote Sensing of Environment* 89 (4): 519–534. doi:10.1016/j.rse.2003.11.008.

Xiao, X. M., D. Pavel, B. Chrashekhar, and B. Eli. 2013. "A Library of Georeferenced Photos from the Field." *EOS Transactions American Geophysical Union* 92 (49): 453–454. doi:10.1029/2011EO490002.

Xiao, X. M., Q. Y. Zhang, D. Hollinger, J. Aber, and B. Moore. 2004b. "Modeling Gross Primary Production of an Evergreen Needleleaf Forest Using MODIS and Climate Data." *Ecological Applications* 15 (3): 954–969. doi:10.1890/04-0470.

Yi, Z.-F., C. H. Cannon, J. Chen, C.-X. Ye, and R. D. Swetnam. 2014. "Developing Indicators of Economic Value and Biodiversity Loss for Rubber Plantations in Xishuangbanna, Southwest China: A Case Study from Menglun Township." *Ecological Indicators* 36: 788–797. doi:10.1016/j.ecolind.2013.03.016.

Yuan, F., K. E. Sawaya, B. C. Loeffelholz, and M. E. Bauer. 2005. "Land Cover Classification and Change Analysis of the Twin Cities (Minnesota) Metropolitan Area by Multitemporal Landsat Remote Sensing." *Remote Sensing of Environment* 98 (2–3): 317–328. doi:10.1016/j.rse.2005.08.006.

Zhu, H., Z. F. Xu, H. Wang, and B. G. Li. 2004. "Tropical Rain Forest Fragmentation and Its Ecological and Species Diversity Changes in Southern Yunnan." *Biodiversity and Conservation* 13 (7): 1355–1372. doi:10.1023/B:BIOC.0000019397.98407.c3.

Zhu, Z., and C. E. Woodcock. 2012. "Object-Based Cloud and Cloud Shadow Detection in Landsat Imagery." *Remote Sensing of Environment* 118 (6): 83–94. doi:10.1016/j.rse.2011.10.028.

Ziegler, A. D., J. M. Fox, and J. C. Xu. 2009. "The Rubber Juggernaut." *Science* 324 (5930): 1024–1025. doi:10.1126/science.1173833.